Supplemental Data

Figure S1

A. Triplex/Csy4 gRNA expression mechanism

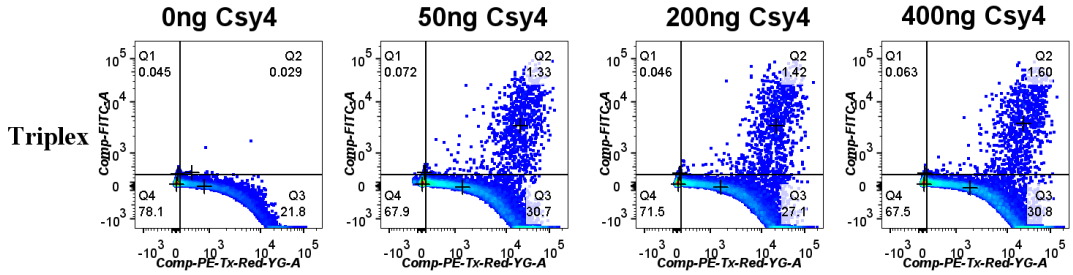

B. Intron/Csy4 gRNA expression mechanism

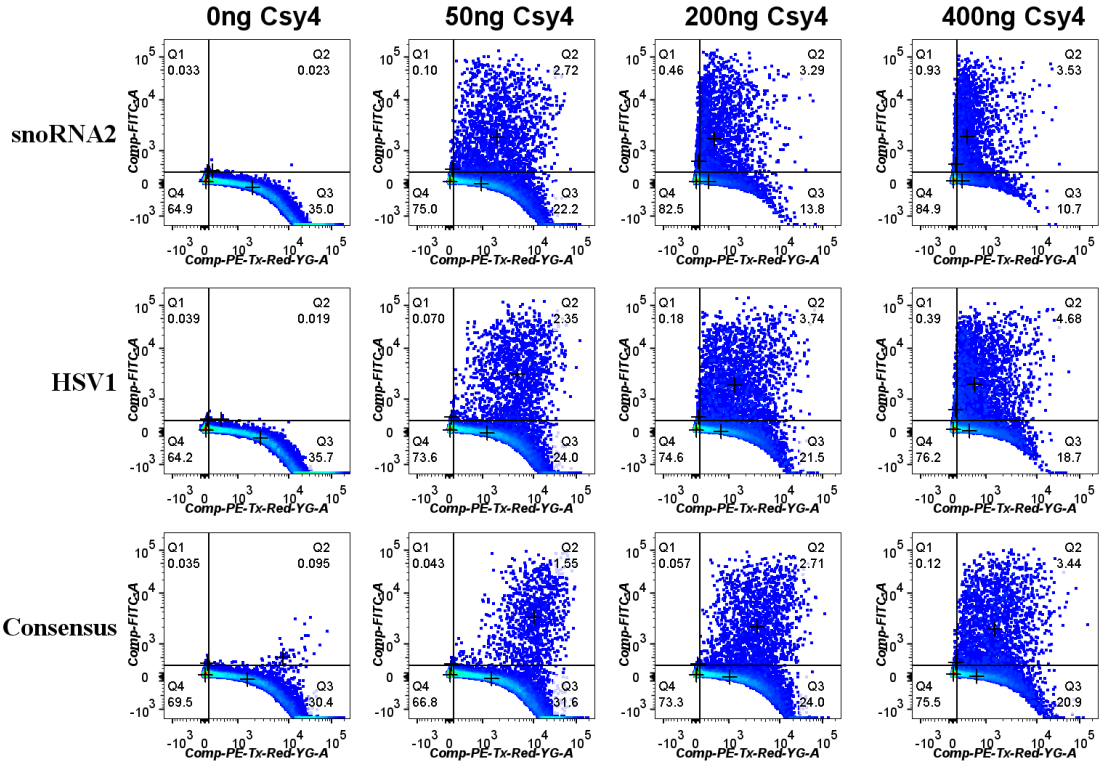

Figure S1. Flow cytometry data corresponding to: **(A)** the 'triplex/Csy4' strategy (Figure 1) and **(B)** the 'intron/Csy4' (Figure 2) strategy for generating functional gRNAs from RNAP II transcripts.

Abbreviations: *Comp-PE-Tx-Red-YG-A* (mKate2); *Comp-FITC-A* (EYFP).

Triplex: construct #3 (CMVp-mK-Tr-28-g1-28, 1 µg).

Consensus, snoRNA2, and HSV1: constructs #8-10, respectively (CMVp-mK_{EX1}-[28-g1-28]$_{'intron\ type'}$-mK_{EX2} with the corresponding intron sequences flanking the gRNA and Csy4 recognition sites ('28')). These plasmids were transfected at 1 µg.

In addition, the amount of the Csy4-expressing plasmid (construct #2) transfected in each sample is indicated. Other plasmids transfected included construct #1 (taCas9, 1 µg) and #5 (P1-EYFP, 1 µg).

Figure S2

A. Triplex/Csy4 mechanism with Cas9 and/or Csy4 controls

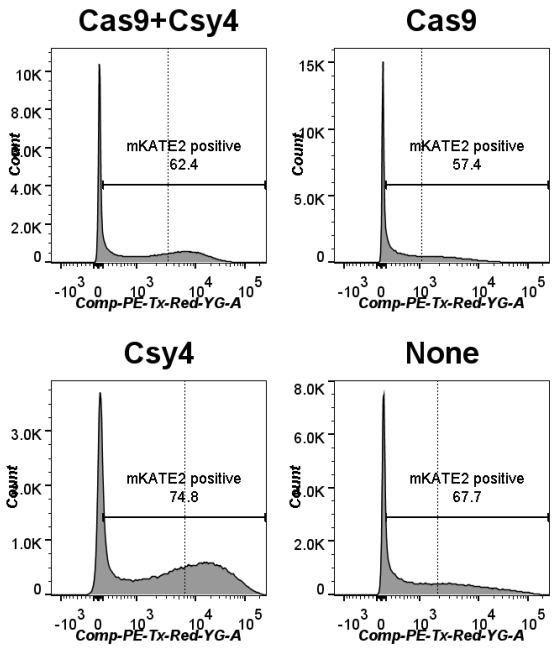

B. Additional controls for the Triplex/Csy4 and Intron/Csy4 mechanisms

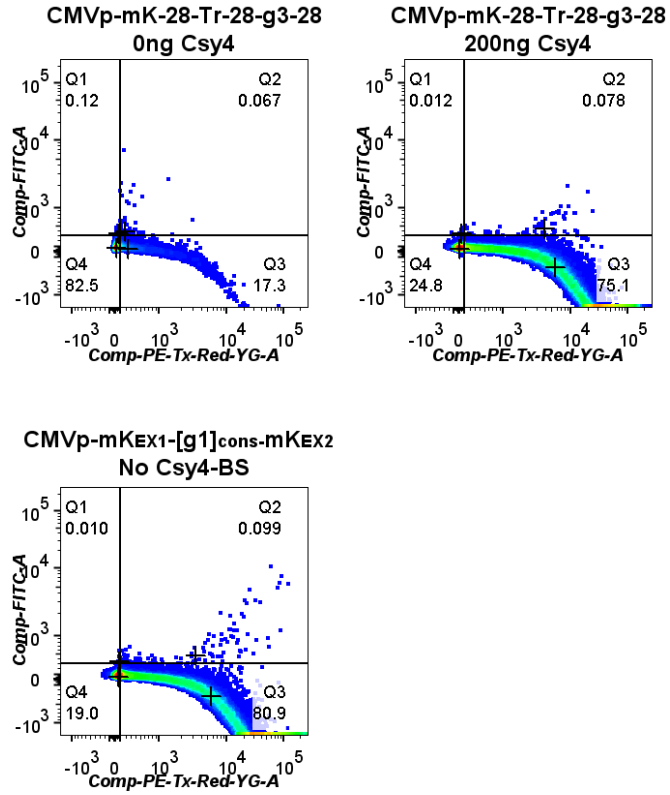

C. Guide RNA crosstalk controls

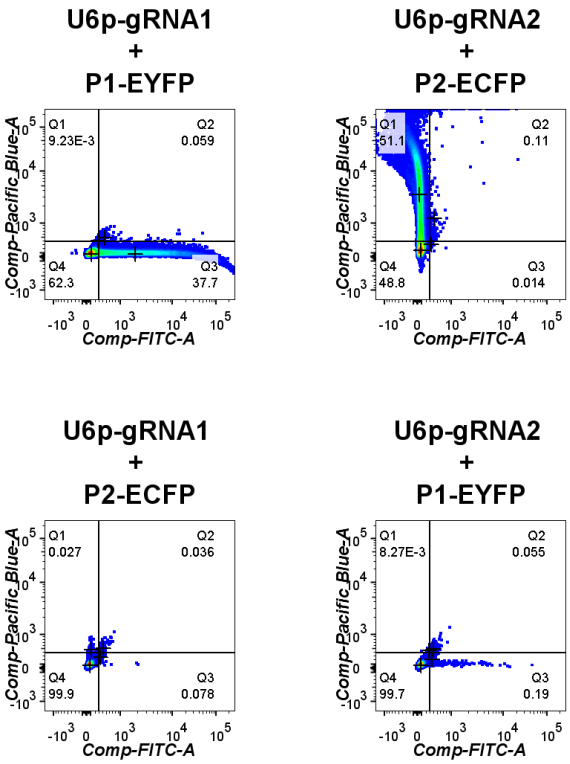

Figure S2. (A) Flow cytometry data corresponding to Figure 1B to analyze how various combinations of Csy4 and taCas9 affect expression of the harboring mKate2 gene for the CMVp-mK-Tr-28-g1-28 architecture. All samples contained Construct #3 (CMVp-mK-Tr-28-g1-28, 1 µg). Construct #1 (taCas9, 1 µg) and Construct #2 (Csy4, 100 ng) were applied as indicated.

(B) Flow cytometry data providing various controls to demonstrate minimal non-specific activation of the P1 promoter by gRNA3 (top two panels) and minimal EYFP activation from the promoter P1 with intronic gRNA1 without Csy4 binding sites (bottom panel). The amount of Csy4 DNA transfected in each sample in the top two panels is indicated. The lower panel (CMVp-mK_{EX1}-$[g1]_{cons}$-mK_{EX2}) was tested in the absence of Csy4. Other plasmids transfected in this experiment included construct #1 (taCas9, 1 µg) and construct #5 (P1-EYFP, 1 µg).

(C) Flow cytometry data corresponding to controls made to validate that no crosstalk exists between gRNA1 and promoter P2 or between gRNA2 and promoter P2. All samples were transfected with the constructs listed in each plot title (1 µg each).

Abbreviations: *Comp-PE-Tx-Red-YG-A* (mKate2)*; Comp-FITC-A* (EYFP); *Comp-Pacific Blue-A* (ECFP).

Figure S3
Exploring the effects of Csy4 recognition site configurations flanking a gRNA

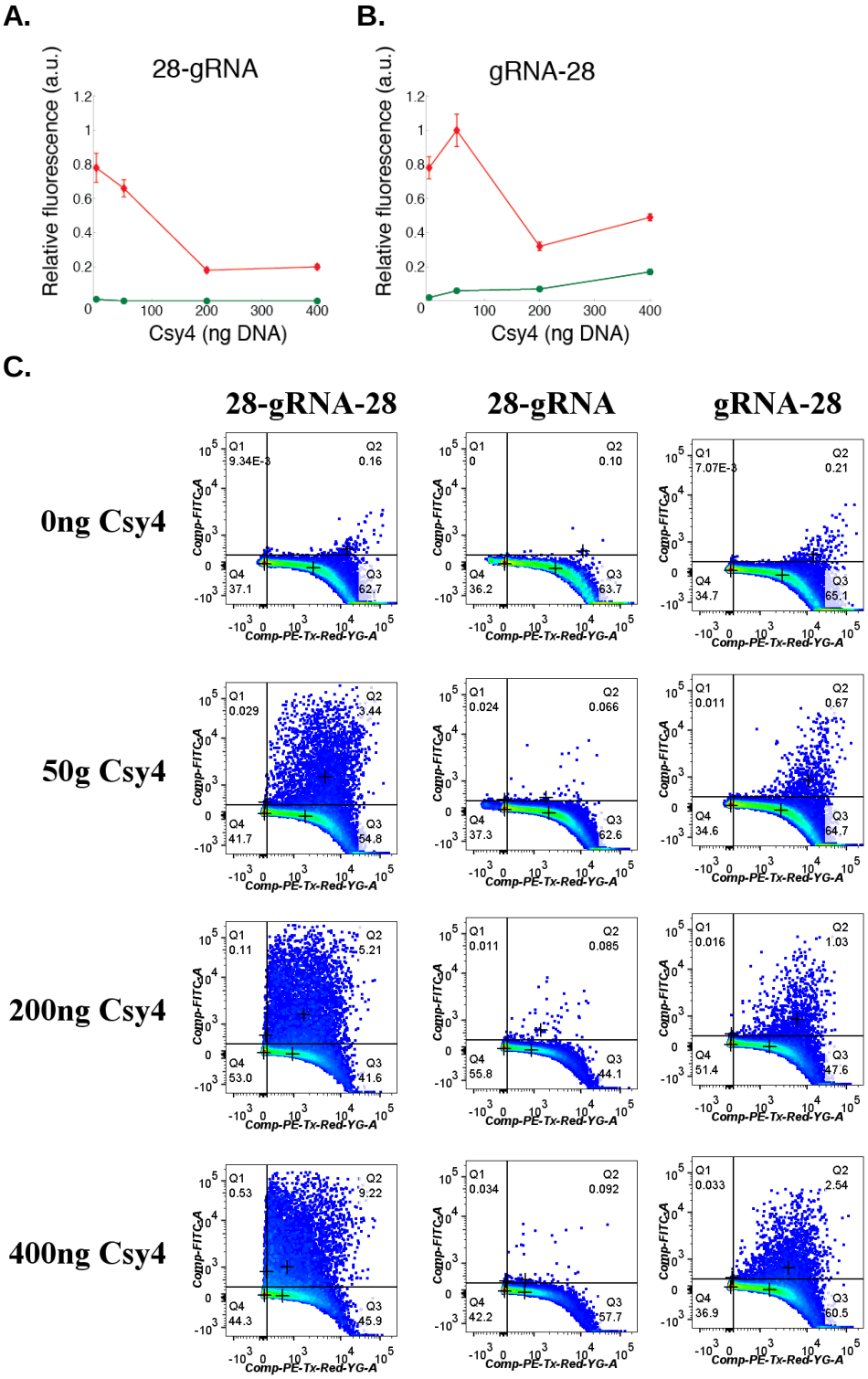

Figure S3. To determine whether both of the 5' and 3' Csy4 recognition sites are necessary for functional gRNA generation from introns, we tested a few variants of the HSV1-based intron within mKate2 (Figure

2A). This intron housed a gRNA1 sequence that was either preceded by a Csy4 binding site on its 5' side ('28-gRNA', Figure S3A) or followed by a Csy4 binding site on its 3' end ('gRNA-28', Figure S3B). The synthetic P1-EYFP construct was used to assess gRNA1 activity. The data for Figure S3A-B was normalized with the performance of the 'intron/Csy4' architecture where the intronic gRNA1 was flanked by two Csy4 binding sites ('28-gRNA-28', Figure S3C). Data are represented as mean +/- SEM.

The single-Csy4-binding-site architectures had mKate2 levels that decreased with the addition of Csy4 (Figure S3A-B). The downstream EYFP activation by the gRNA1-directed CRISPR-TF was significantly lower for the single Csy4-binding-site architectures (Figure S3A-B) versus the 'intron/Csy4' construct (Figure 2D and Figure S3C). When only one Csy4 binding site was located at the 5' end of the gRNA1 intron, EYFP expression was nearly undetectable (Figure S3A). When only one Csy4 binding site was located at the 3' end of the gRNA1 intron, a 6-fold reduction in EYFP levels was observed (Figure S3B) compared with the 'intron/Cys4' architecture that contains two Csy4 recognition sites flanking gRNA1 (Figure 2D and Figure S3C).

These results demonstrate that while the 5' Csy4 recognition sequence is important for generating functional intronic gRNAs, the 3' Csy4 binding site is essential. We hypothesize that Csy4 can help stabilize intronic gRNA through several potential mechanisms. The 5' end of RNAs cleaved by Csy4 contain a hydroxyl (OH^-) which may protect them from major 5'→3' cellular RNases such as the XRN family, which require a 5' phosphate for substrate recognition (Houseley and Tollervey, 2009; Nagarajan et al., 2013). In addition, binding of the Csy4 protein to the 3' end of the cleaved gRNA (Haurwitz et al., 2012) may protect it from 3'→5' degradation mediated by the eukaryotic exosome complex (Houseley and Tollervey, 2009).

Figure S3C shows the flow cytometry data for analyzing how the various configurations of Csy4 recognition sites flanking the gRNA within the HSV1 intron affect CRISPR-TF activity. The fluorescence values for Figure S3A and S3B were normalized to the maximum fluorescence levels between these experiments and the $[28\text{-}g1\text{-}28]_{HSV1}$ control (Figure S3C).

Abbreviations: *Comp-PE-Tx-Red-YG-A* (mKate2); *Comp-FITC-A* (EYFP).

'28-gRNA-28' is HSV1 intronic gRNA flanked by two Csy4 recognition sites (construct #4, CMVp-mK_{EX1}-$[28\text{-}g1\text{-}28]_{HSV1}$-$mK_{EX2}$)
'28-gRNA' is HSV1 intronic gRNA with a 5' Csy4 recognition site only (construct #10, CMVp-mK_{EX1}-$[28\text{-}g1]_{HSV1}$-mK_{EX2})
'gRNA-28' is HSV1 intronic gRNA with a 3' Csy4 recognition site only (construct #11, CMVp-mK_{EX1}-$[g1\text{-}28]_{HSV1}$-mK_{EX2}).

In addition, the amount of the Csy4-expressing plasmid transfected in each sample is indicated with each figure. Other plasmids transfected in this experiment include construct #1 (taCas9, 1 µg) and construct #5 (P1-EYFP 1 µg).

Figure S4
Engineering ribozymes to release functional gRNAs from RNAP II transcripts

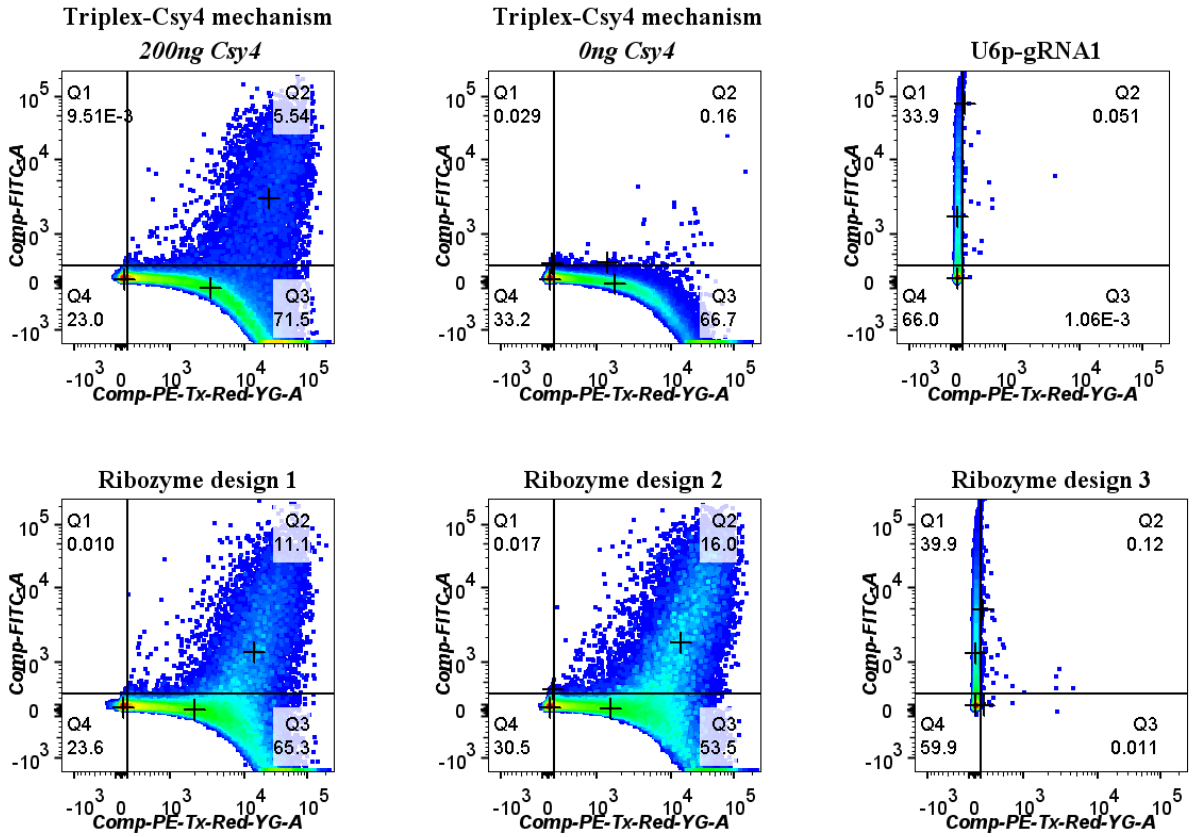

Figure S4. Flow cytometry data corresponding to Figure 3.

Abbreviations: *Comp-PE-Tx-Red-YG-A* (mKate2); *Comp-FITC-A* (EYFP).

'Triplex-Csy4' mechanism contains construct #3 (CMVp-mK-Tr-28-g1-28). Other plasmids transfected in this experiment include construct #1 (taCas9, 1 µg); construct #5 (P1-EYFP); construct #2 (Csy4, concentrations indicated).

'Ribozyme design 1' contains construct #13 (CMVp-mK-Tr-HH-g1-HDV). Other plasmids transfected in this experiment include construct #1 (taCas9, 1 µg); construct #5 (P1-EYFP, 1 µg).

'Ribozyme design 2' contains construct #14 (CMVp-mK-HH-g1-HD). Other plasmids transfected in this experiment include construct #1 (taCas9, 1 µg); construct #5 (P1-EYFP, 1 µg).

'Ribozyme design 3' contains construct #15 (CMVp-HH-g1-HDV). Other plasmids transfected in this experiment include construct #1 (taCas9, 1 µg); construct #5 (P1-EYFP, 1 µg).

'U6p-gRNA1' contains construct #7 (U6p-g1, 1 µg). Other plasmids transfected in this experiment include construct #1 (taCas9, 1 µg).

Figure S5
Multiplexed expression of 2x gRNAs from a single transcript

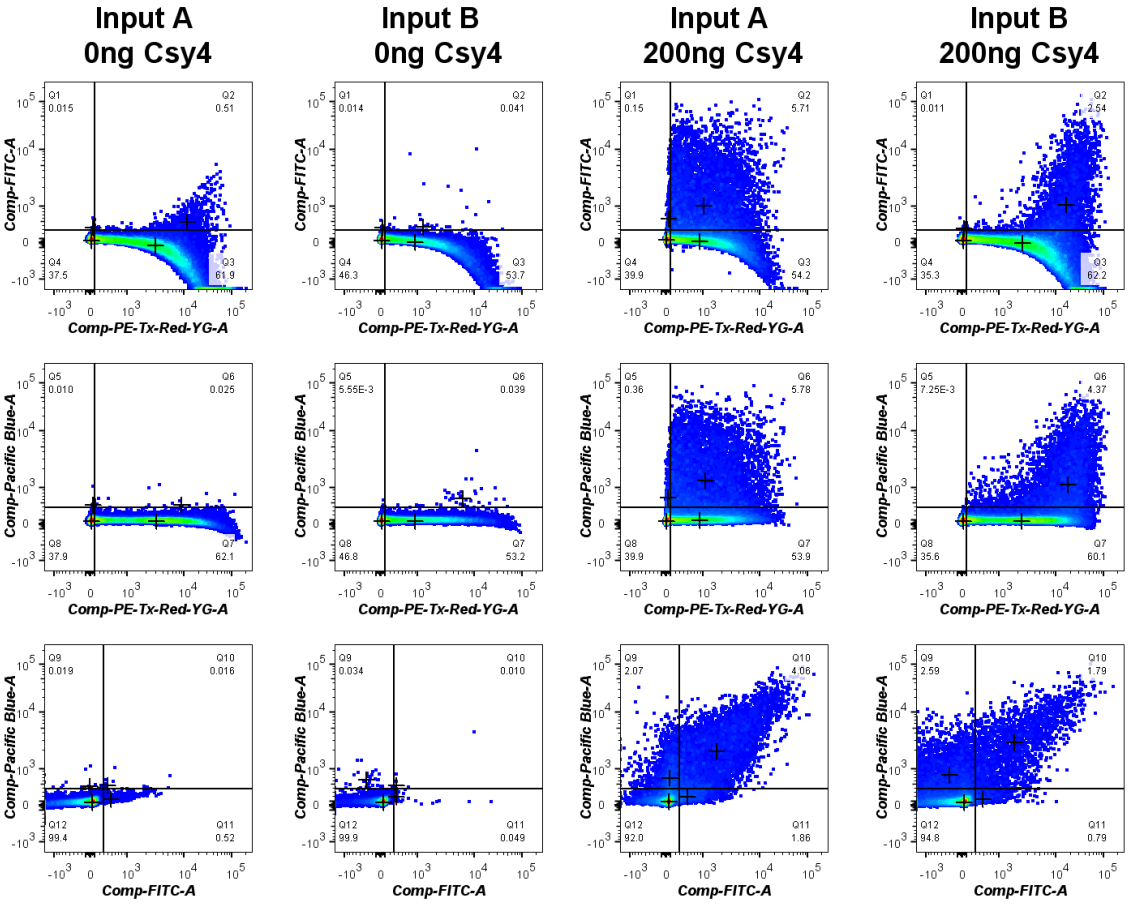

Figure S5. Flow cytometry data corresponding to Figure 4.

Abbreviations: *Comp-PE-Tx-Red-YG-A* (mKate2); *Comp-FITC-A* (EYFP); *Comp-Pacific Blue-A* (ECFP).

'Input A' refers to the 'intron-triplex' architecture and contains constructs #16 (CMVp-mK$_{EX1}$-[28-g1-28]$_{HSV1}$-mK$_{EX2}$-Tr-28-g2-28, 1 µg); #5 (P1-EYFP, 1 µg); #6 (P2-ECFP, 1 µg); and #1 (taCas9, 1 µg), as shown in Figure 4A.

'Input B' refers to the 'triplex-tandem' architecture and contains constructs #17 (CMVp-mK-Tr-28-g1-28-g2-28, 1 µg); #5 (P1-EYFP, 1 µg) and #6 (P2-ECFP, 1 µg); and #1 (taCas9, 1 µg), as shown in Figure 4B.

In addition, the amount of Csy4-expressing plasmid DNA (Construct #2) transfected in each sample is indicated above each plot.

Figure S6
Synthetic transcriptional cascades

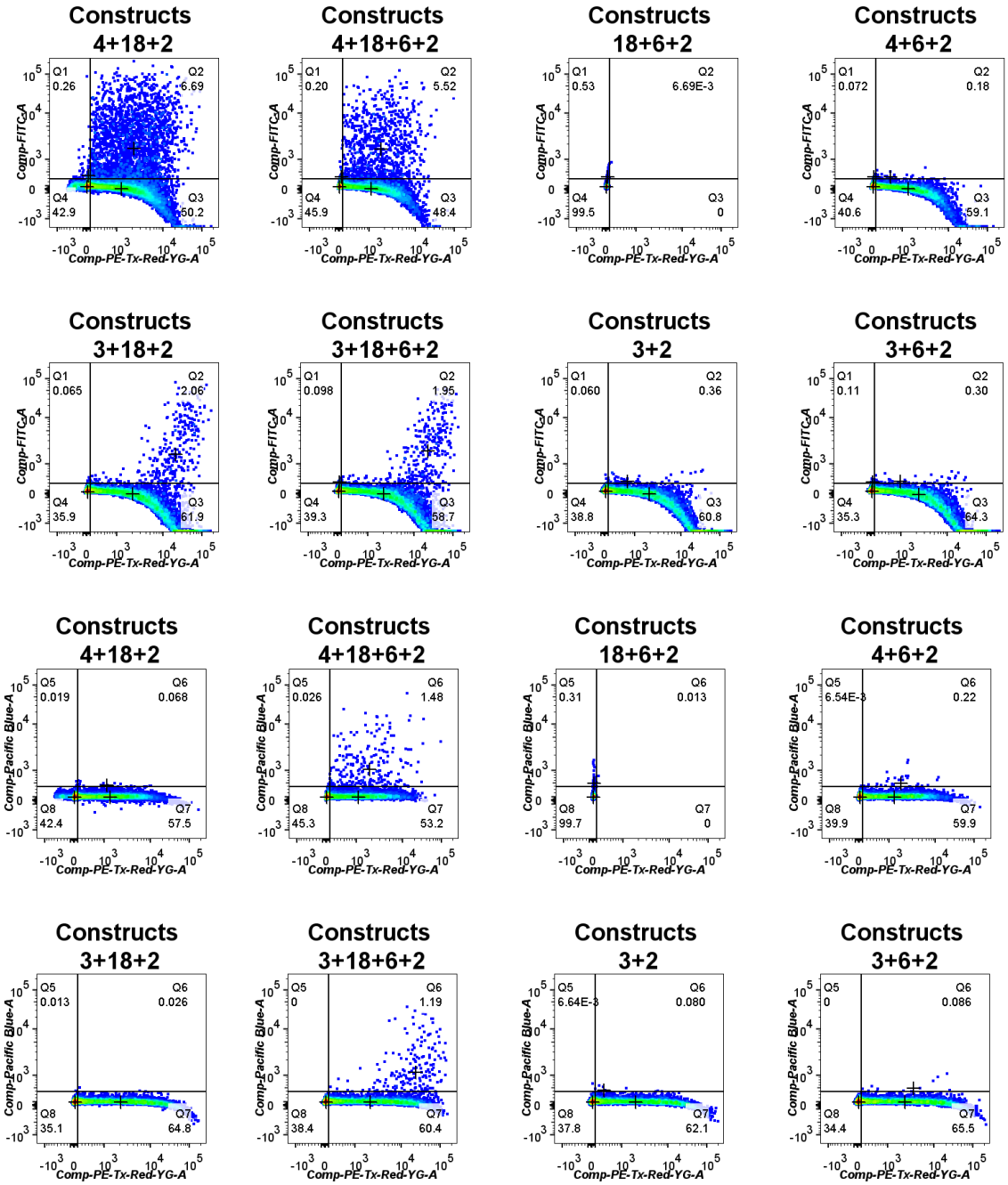

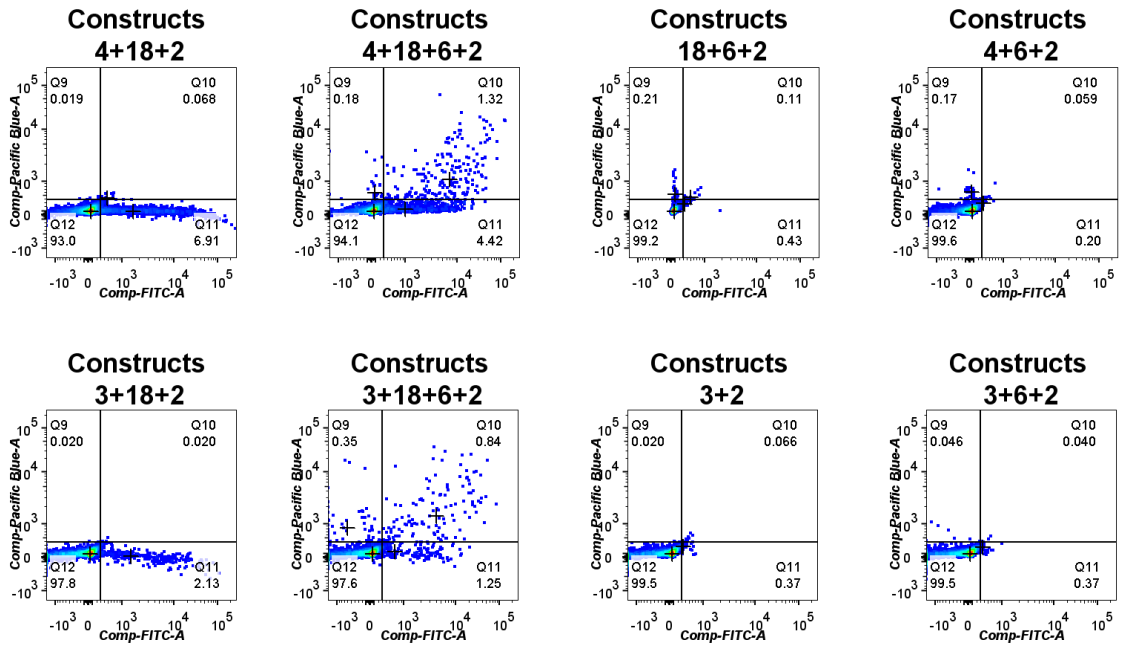

Figure S6. Flow cytometry data corresponding to Figure 6.

Abbreviations: *Comp-PE-Tx-Red-YG-A* (mKate2); *Comp-FITC-A* (EYFP); *Comp-Pacific Blue-A* (ECFP).

All samples were transfected with the constructs listed in each plot title (1 µg each, Table S1) and 200 ng of the Csy4-expressing plasmid (construct #2).

Figure S7
Rewiring synthetic circuit interconnections with Csy4

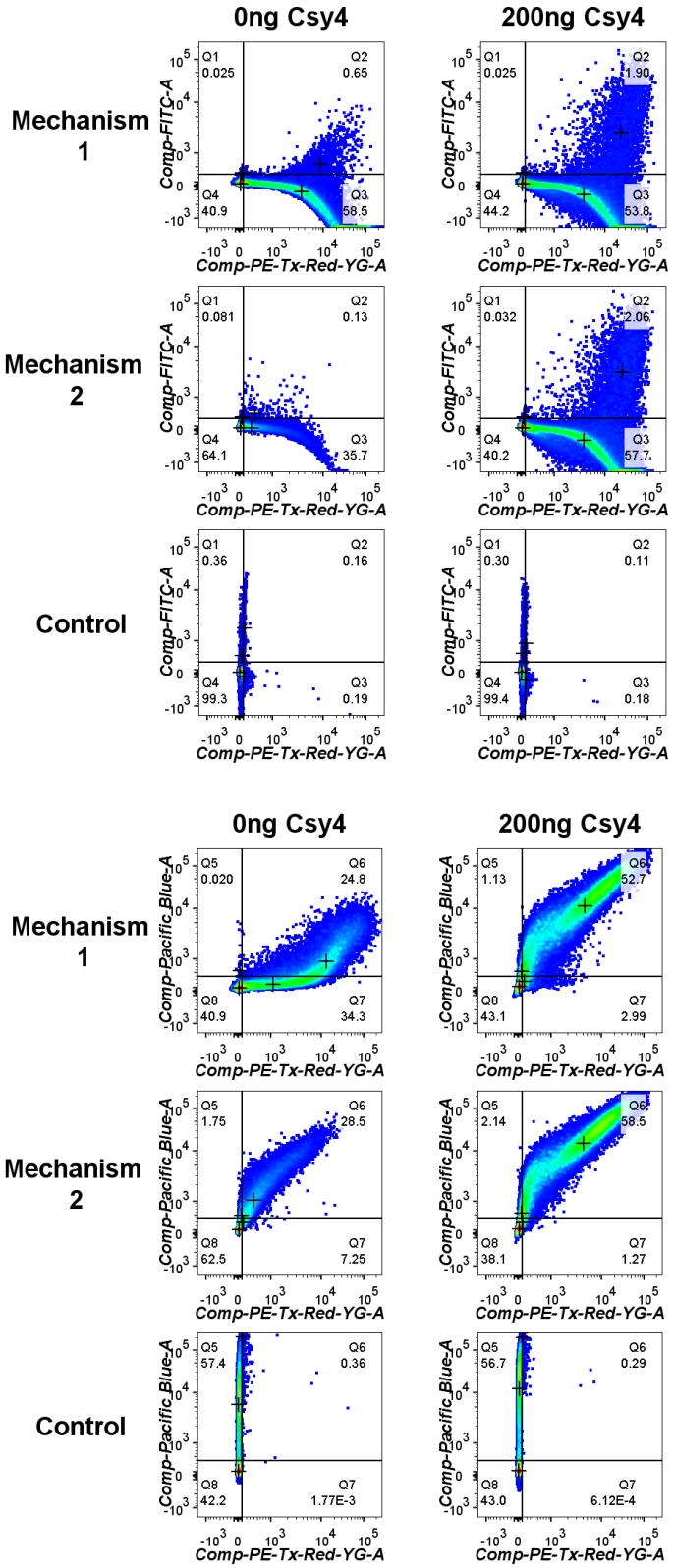

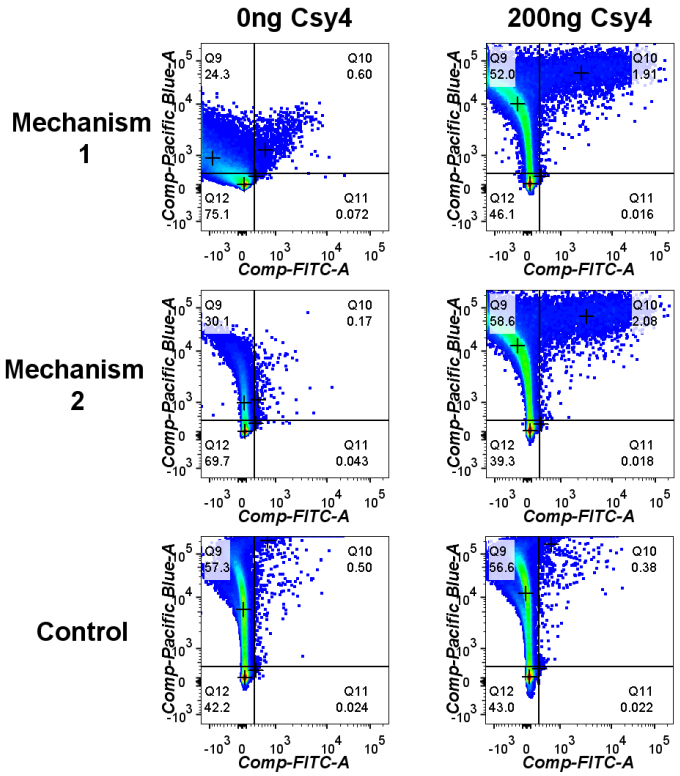

Figure S7. Flow cytometry data corresponding to Figure 7.

Abbreviations: *Comp-PE-Tx-Red-YG-A* (mKate2); *Comp-FITC-A* (EYFP); *Comp-Pacific Blue-A* (ECFP).

'Mechanism 1' contains the following constructs: #20 (CMVp-mK$_{Ex1}$-[miR]-mK$_{Ex2}$-Tr-28-g1-28); #22 (CMVp-ECFP-Tr-28-miR$_{8xBS}$-28); and #5 (P1-EYFP). These plasmids were transfected at a concentration of 1 µg each. This mechanism corresponds to the circuit diagram in Figure 7A.

'Mechanism 2' contains the following constructs: #21 (CMVp-mK$_{Ex1}$-[miR]-mK$_{Ex2}$-Tr-28-g1-28-miR$_{4xBS}$); #22 (CMVp-ECFP-Tr-28-miR$_{8xBS}$-28); and #5 (P1-EYFP). These plasmids were transfected at a concentration of 1 µg each. This mechanism corresponds to the circuit diagram in Figure 7D.

'Control' samples contain constructs #22 (CMVp-ECFP-Tr-28-miR$_{8xBS}$-28) and #5 (P1-EYFP) only. These plasmids were transfected at a concentration of 1 µg each.

In addition, the amount of Csy4-expressing plasmid (Construct #2) transfected in each sample is indicated above each plot.

Table S1. Construct names, designs, and abbreviations

Construct 1	**CMVp-dCas9-3xNLS-VP64-3'LTR**
Abbreviation	taCas9
Construct 2	**PGK1p-Csy4-pA**
Abbreviation	Csy4
Construct 3	**CMVp-mKate2-Triplex-28-gRNA1-28-pA**
Abbreviation	CMVp-mK-Tr-28-g1-28
Construct 4	**CMVp-mKate2_EX1-[28-gRNA1-28]$_{HSV1}$-mKate2_EX2-pA**
Abbreviation	CMVp-mK$_{EX1}$-[28-g1-28]$_{HSV1}$-mK$_{EX2}$
Construct 5	**P1-EYFP-pA**
Abbreviation	P1-EYFP
Construct 6	**P2-ECFP-pA**
Abbreviation	P2-ECFP
Construct 7	**U6p-gRNA1-TTTTT**
Abbreviation	U6p-g1
Construct 8	**CMVp-mKate2_EX1-[28-gRNA1-28]$_{consensus}$-mKate2_EX2-pA**
Abbreviation	CMVp-mK$_{EX1}$-[28-g1-28]$_{cons}$-mK$_{EX2}$
Construct 9	**CMVp-mKate2_EX1-[28-gRNA1-28]$_{snoRNA2}$-mKate2_EX2-pA**
Abbreviation	CMVp-mK$_{Ex1}$-[28-g1-28]$_{sno}$-mK$_{Ex2}$
Construct 10	**CMVp-mKate2_EX1-[28-gRNA1]$_{HSV1}$-mKate2_EX2-pA**
Abbreviation	CMVp-mK$_{EX1}$-[28-g1]$_{HSV1}$-mK$_{EX2}$
Construct 11	**CMVp-mKate2_EX1-[gRNA1-28]$_{HSV1}$-mKate2_EX2-pA**
Abbreviation	CMVp-mK$_{EX1}$-[g1-28]$_{HSV1}$-mK$_{EX2}$
Construct 12	**CMVp-mKate2_EX1-[gRNA1]$_{consensus}$-mKate2_EX2-pA**
Abbreviation	CMVp-mK$_{EX1}$-[g1]$_{cons}$-mK$_{EX2}$
Construct 13	**CMVp-mKate2-Triplex-HHRibo-gRNA1-HDVRibo-pA**
Abbreviation	CMVp-mK-Tr-HH-g1-HDV
Construct 14	**CMVp-mKate2-HHRibo-gRNA1-HDVRibo-pA**
Abbreviation	CMVp-mK-HH-g1-HDV
Construct 15	**CMVp-HHRibo-gRNA1-HDVRibo-pA**

Abbreviation	CMVp-HH-g1-HDV
Construct 16	**CMVp-mKate2_EX1-[28-gRNA1-28]$_{HSV1}$-mKate2_EX2-Triplex-28-gRNA2-28-pA**
Abbreviation	CMVp-mK$_{EX1}$-[28-g1-28]$_{HSV1}$-mK$_{EX2}$-Tr-28-g2-28
Construct 17	**CMVp-mKate2-Triplex-28-gRNA1-28-gRNA2-28-pA**
Abbreviation	CMVp-mK-Tr-28-g1-28-g2-28
Construct 18	**P1-EYFP-Triplex-28-gRNA2-28-pA**
Abbreviation	P1-EYFP-Tr-28-g2-28
Construct 19	**CMVp-mKate2-Triplex-28-gRNA3-28-gRNA4-28-gRNA5-28-gRNA6-28-pA**
Abbreviation	CMVp-mK-Tr-(28-g-28)$_{3-6}$
Construct 20	**CMVp-mKate2_EX1-[miRNA]-mKate2_EX2-Triplex-28-gRNA1-28-pA**
Abbreviation	CMVp-mK$_{EX1}$-[miR]-mK$_{EX2}$-Tr-28-g1-28
Construct 21	**CMVp-mKate2_EX1-[miRNA]-mKate2_EX2-Triplex-28-gRNA1-28-4xmiRNA-BS-pA**
Abbreviation	CMVp-mK$_{EX1}$-[miR]-mK$_{EX2}$-Tr-28-g1-28-miR$_{4xBS}$
Construct 22	**CMVp-ECFP-Triplex-28-8xmiRNA-BS-28-pA**
Abbreviation	CMVp-ECFP-Tr-28-miR$_{8xBS}$-28
Construct 23	**CMVp-mKate2-Triplex-28-gRNA3-28**
Abbreviation	CMVp-mK-Tr-28-g3-28
Construct 24	**CMVp-mKate2-Triplex-28-gRNA4-28**
Abbreviation	CMVp-mK-Tr-28-g4-28
Construct 25	**CMVp-mKate2-Triplex-28-gRNA5-28**
Abbreviation	CMVp-mK-Tr-28-g5-28
Construct 26	**CMVp-mKate2-Triplex-28-gRNA6-28**
Abbreviation	CMVp-mK-Tr-28-g6-28

Extended Experimental Procedures

Compensation controls

Compensation controls were strict and designed to remove false-positive cells even at the cost of removing true-positive cells. Compensation was done with BD FACSDiva (version no. 6.1.3; BD Biosciences) as detailed below:

Table S3. Compensation setup for flow cytometry

Fluorochrome	-% Fluorochrome	Spectral Overlap
PE-Tx-Red-YG	FITC	0%
Pacific Blue	FITC	0.2%
FITC	PE-Tx-Red-YG	21.1%
Pacific Blue	PE-Tx-Red-YG	1%
FITC	Pacific Blue	7.5%

Flow cytometry analysis

Compensated flow cytometry results were analyzed using FlowJo software (vX.0.7r2). Calculations were performed as described below:

1. All samples were gated to exclude cell clumps and debris (population P1)

2. Histograms of P1 cells were analyzed according to the following gates, which were determined according to the auto-fluorescence of non-transfected cells in the same acquisition conditions such that the proportion of false-positive cells would be lower than 0.1%:
    a. mKate2: ‘mKate2 positive’ cells were defined as cells above a fluorescence threshold of 100 a.u.
    b. EYFP: ‘EYFP positive’ cells were defined as cells above a fluorescence threshold of 300 a.u.
    c. ECFP: ‘ECFP positive’ cells were defined as cells above a fluorescence threshold of 400 a.u.

3. The percent of positive cells (% positive) and the median fluorescence for each ‘positive cell’ population were calculated. The % positive cells was multiplied by the median fluorescence, resulting in a weighted median fluorescence expression level that correlated fluorescence intensity with cell numbers. This measurement strategy is consistent with several previous studies (Auslander et al., 2012; Xie et al., 2011).

4. The weighted median fluorescence was determined for each sample. The mean of the weighted median fluorescence of biological triplicates was calculated. These are the data presented in the paper. The standard error of the mean (SEM) was also computed and presented as error bars.

5. To facilitate comparisons between various constructs and to account for variations in the brightness of different fluorescent proteins, the weighted median fluorescence for each experimental condition was divided by the maximum weighted median fluorescence for the same fluorophore among all conditions tested in the same set of experiments.

Flow cytometry data plots shown in the Supplemental information are representative compensated data from a single experiment. As noted above, cells were gated to exclude cell clumps and debris (population P1), and the entire gated population of viable cells are presented in each figure. The threshold for each sub-population Q1-Q4 was set according to the thresholds described above. The percentage of cells in each sub-population is indicated in the plots. Black crosses in the plots indicate the median fluorescence for a specific sub-population.

Plasmid construction

The plasmid **CMVp-mKate2-Triplex-28-gRNA1-28-pA** (Construct 3, Table S1) was built using Gibson Assembly from three parts amplified with appropriate homology overhangs: 1) the full length coding sequence of mKate2; 2) the first 110 bp of the mouse MALAT1 3' triple helix (Wilusz et al., 2012); and 3) gRNA1 containing a 20 bp Specificity Determining Sequence (SDS) and a *S. pyogenes* gRNA scaffold along with 28nt Csy4 recognition sites.

The reporter plasmids **P1-EFYP-pA** (Construct 5, Table S1) and **P2-ECFP-pA** (Construct 6, Table S1) were built by cloning in repeated gRNA1 binding sites and repeated gRNA2 binding sites into the NheI site of **pG5-Luc** (Promega) via annealing complementary oligonucleotides. Then, EYFP and ECFP were cloned into the NcoI/FseI sites, respectively.

The plasmid **CMVp-mKate2_EX1-[28-gRNA1-28]$_{HSV1}$-mKate2_EX2-pA** (Construct 4, Table S1) was built by Gibson Assembly of the following parts with appropriate homology overhangs: 1) the mKate2_EX1 (a.a. 1-90) of mKate2; 2) mKate_EX2 (a.a. 91-239) of mKate2; and 3) gRNA1 containing a 20bp SDS followed by the *S. pyogenes*

gRNA scaffold flanked by Csy4 recognition sites and the HSV1 acceptor, donor and branching sequences. Variations of the **CMVp-mKate2_EX1-[28-gRNA1-28]$_{HSV1}$-mKate2_EX2-pA** plasmid containing consensus and SnoRNA2 acceptor, donor, and branching sequences and with and without the Csy4 recognition sequences (Constructs 8-12, Table S1) were built in a similar fashion.

The ribozyme-expressing plasmids **CMVp-mKate2-Triplex-HHRibo-gRNA1-HDVRibo-pA** and **CMVp-mKate2-HHRibo-gRNA1-HDVRibo-pA** plasmids (Constructs 13 and 14, respectively, Table S1) were built by Gibson Assembly of XmaI-digested **CMVp-mKate2**, and PCR-extended amplicons of gRNA1 (with and without the triplex and containing HHRibo (Gao and Zhao, 2014) on the 5' end and HDVRibo (Gao and Zhao, 2014) on the 3' end). The plasmid **CMVp-HHRibo-gRNA1-HDVRibo-pA** (Construct 15, Table S1) was built similarly by Gibson Assembly of SacI-digested **CMVp-mKate2** and a PCR-extended amplicon of gRNA1 containing HHRibo on the 5' end and HDVRibo on the 3' end.

The plasmid **CMVp-mKate2_EX1-[28-gRNA1-28]$_{HSV1}$-mKate2_EX2-Triplex-28-gRNA2-28-pA** (Construct 16, Table S1) was built by Gibson Assembly of the following parts using appropriate homologies: 1) XmaI-digested **CMVp-mKate2_EX1-[28-gRNA1-28]$_{HSV1}$-mKate2_EX2-pA** (Construct 4, Table S1) and 2) PCR amplified Triplex-28-gRNA2-28 from **CMVp-mKate2-Triplex-28-gRNA1-28-pA** (Construct 3, Table S1).

The plasmid **CMVp-mKate2-Triplex-28-gRNA1-28-gRNA2-28-pA** (Construct 17, Table S1) was built by Gibson Assembly with the following parts using appropriate homologies: 1) XmaI-digested **CMVp-mKate2-Triplex-28-gRNA1-28-pA** (Construct 3, Table S1) and 2) PCR amplified 28-gRNA2-28.

The plasmid **CMVp-mKate2-Triplex-28-gRNA3-28-gRNA4-28-gRNA5-28-gRNA6-28-pA** (Construct 19, Table S1) was constructed using a Golden Gate approach using the Type IIs restriction enzyme, BsaI (Engler and Marillonnet, 2013), as shown below:

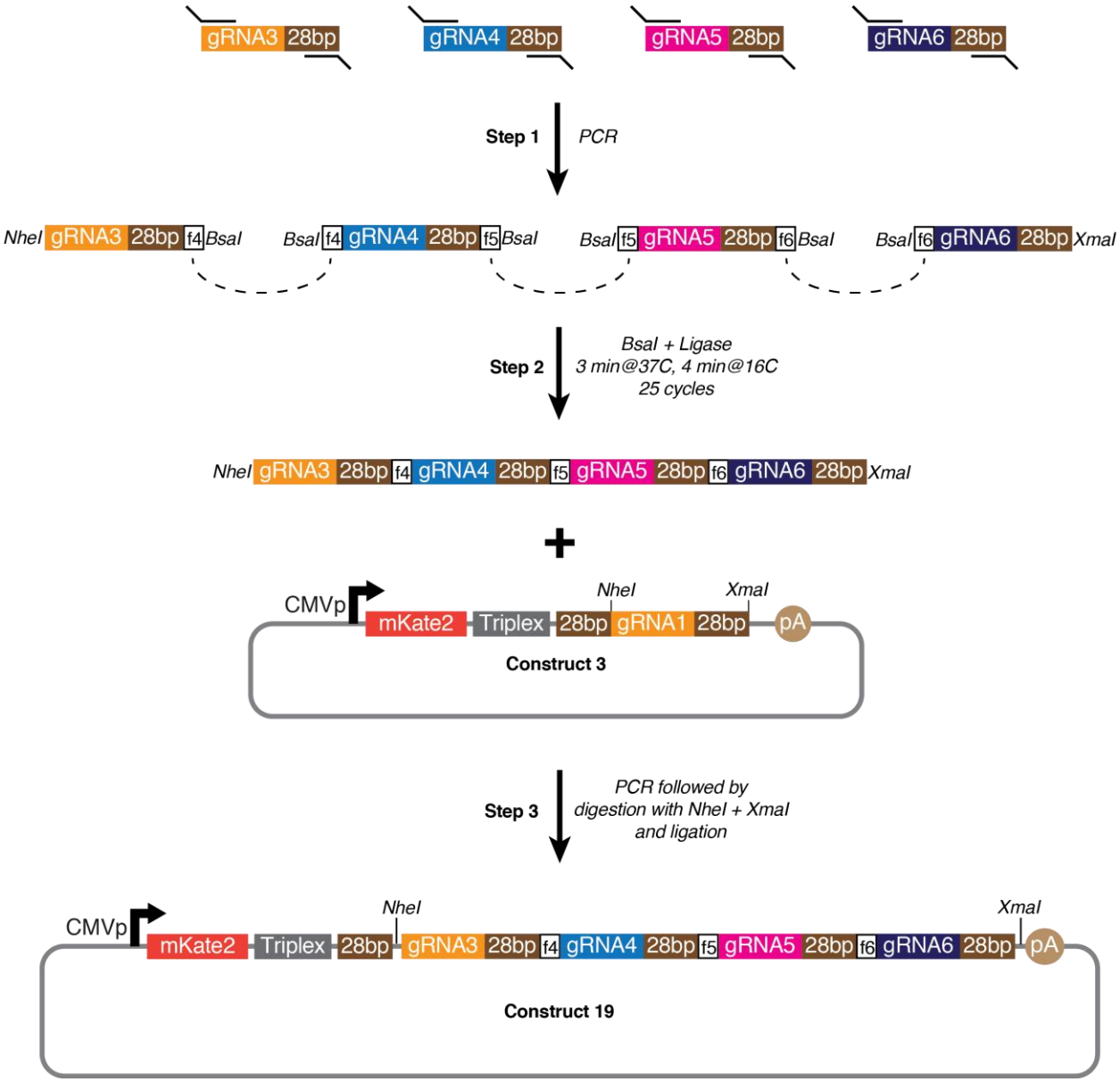

Step 1 – Each individual gRNA of interest (e.g., gRNA3, gRNA4, etc.) containing a 20 bp SDS followed by the *S. pyogenes* gRNA scaffold and a Csy4 '28' sequence was PCR amplified to be flanked on both the 5' and 3' ends by the BsaI type IIs restriction enzyme site. Short, 5 base pair sequences (e.g., f3, f4, etc.) were introduced on the 5' and 3' ends immediately downstream and upstream of the BsaI sites, respectively. These 5 bp sequences were designed

such that each adjoining gRNA to be cloned would contain the same 5 bp sequence.

Step 2 – The amplified products containing the BsaI sites were mixed in a single reaction mixture containing the enzyme BsaI and T4 DNA ligase. The reaction mixture was subjected to 25 repeats of 3 minute digestions followed by 4 minute ligations at 37°C and 16°C, respectively.

Step 3 – The assembled product containing all the gRNAs of interest from Step 2 was further PCR amplified to produce a larger amount of the assembled gRNA construct. This product was then digested with NheI-HF and XmaI and cloned into the **CMVp-mKate2-Triplex-28-gRNA1-28-pA** plasmid (Construct 3, Table S1).

The CMVp-mKate2_EX1-[miRNA]-mKate2_EX2-pA plasmid containing an intronic FF4 (a synthetic miRNA) was received as a gift from Lila Wroblewska. The synthetic FF4 miRNA was cloned into an intron with consensus acceptor, donor and branching sequences between a.a. 90 and 91 of mKate2 to create **CMVp-mKate2_EX1-[miRNA]-mKate2_EX2-Triplex-28-gRNA1-28-pA** (Construct 20, Table S1) and **CMVp-mKate2_EX1-[miRNA]-mKate2_EX2-Triplex-28-gRNA1-28-4xmiRNA-BS-pA** (Construct 21, Table S1).

The plasmid **CMVp-ECFP-Triplex-28-8xmiRNA-BS-28-pA** (Construct 22, Table S1) was cloned via Gibson Assembly with the following parts: 1) full length coding sequence of ECFP and 2) 110 nt of the MALAT1 3’ triple helix sequence amplified via PCR extension with oligonucleotides containing eight FF4 miRNA binding sites and Csy4 recognition sequences on both ends. Cloning protocol for multiplexed gRNA expression constructs

Quantitative reverse transcription–PCR (RT-PCR)

The experimental procedure followed was as described in (Perez-Pinera et al., 2013). Cells were harvested 72h post-transfection. Total RNA was isolated by using the RNeasy Plus RNA isolation kit (Qiagen). cDNA synthesis was performed by using qScript cDNA SuperMix (Quanta Biosciences). Real-time PCR using PerfeCTa SYBR Green FastMix (Quanta Biosciences) was performed with the Mastercycler ep realplex real-time PCR system (Eppendorf) with oligonucleotide primers, which were as follows:

IL1RN: forward GGAATCCATGGAGGGAAGAT
reverse TGTTCTCGCTCAGGTCAGTG

GAPDH: forward CAATGACCCCTTCATTGACC
reverse TTGATTTTGGAGGGATCTCG

The primers were designed using Primer3Plus software and purchased from IDT. Melting curve analysis was used to confirm primer specificity. To ensure linearity of the standard curve, reaction efficiencies over the appropriate dynamic range were calculated. Using the ddCt method, we calculated fold-increases in the mRNA expression of the gene of interest normalized to GAPDH expression. We then normalized the mRNA levels to the non-specific gRNA1 control condition. Reported values are the means of three independent biological replicates with technical duplicates that were averaged for each experiment. Error bars represent standard error of the mean (SEM).

Supplemental References

Auslander, S., Auslander, D., Muller, M., Wieland, M., and Fussenegger, M. (2012). Programmable single-cell mammalian biocomputers. Nature *487*, 123-127.

Engler, C., and Marillonnet, S. (2013). Combinatorial DNA assembly using Golden Gate cloning. Methods in molecular biology (Clifton, NJ) *1073*, 141-156.

Gao, Y., and Zhao, Y. (2014). Self-processing of ribozyme-flanked RNAs into guide RNAs in vitro and in vivo for CRISPR-mediated genome editing. Journal of Integrative Plant Biology, n/a-n/a.

Haurwitz, R.E., Sternberg, S.H., and Doudna, J.A. (2012). Csy4 relies on an unusual catalytic dyad to position and cleave CRISPR RNA. Embo j *31*, 2824-2832.

Houseley, J., and Tollervey, D. (2009). The Many Pathways of RNA Degradation. Cell *136*, 763-776.

Nagarajan, V.K., Jones, C.I., Newbury, S.F., and Green, P.J. (2013). XRN 5′->3′ exoribonucleases: Structure, mechanisms and functions. Biochimica et Biophysica Acta (BBA) - Gene Regulatory Mechanisms *1829*, 590-603.

Perez-Pinera, P., Kocak, D.D., Vockley, C.M., Adler, A.F., Kabadi, A.M., Polstein, L.R., Thakore, P.I., Glass, K.A., Ousterout, D.G., Leong, K.W.*, et al.* (2013). RNA-guided gene activation by CRISPR-Cas9-based transcription factors. Nat Meth *10*, 973-976.

Wilusz, J.E., JnBaptiste, C.K., Lu, L.Y., Kuhn, C.D., Joshua-Tor, L., and Sharp, P.A. (2012). A triple helix stabilizes the 3' ends of long noncoding RNAs that lack poly(A) tails. Genes & development *26*, 2392-2407.

Xie, Z., Wroblewska, L., Prochazka, L., Weiss, R., and Benenson, Y. (2011). Multi-Input RNAi-Based Logic Circuit for Identification of Specific Cancer Cells. Science *333*, 1307-1311.